Talanta 130 (2014) 198–206

Contents lists available at ScienceDirect

Talanta

journal homepage: www.elsevier.com/locate/talanta

Poly(brilliant green) and poly(thionine) modified carbon nanotube coated carbon film electrodes for glucose and uric acid biosensors

M. Emilia Ghica, Christopher M.A. Brett*

Departamento de Química, Faculdade de Ciências e Tecnologia, Universidade de Coimbra, 3004-535 Coimbra, Portugal

ARTICLE INFO

Article history:
Received 22 April 2014
Received in revised form
25 June 2014
Accepted 28 June 2014
Available online 5 July 2014

Keywords:
Poly(brilliant green)
Poly(thionine)
Carbon film electrodes
Carbon nanotubes
Glucose oxidase
Uricase

ABSTRACT

Poly(brilliant green) (PBG) and poly(thionine) (PTH) films have been formed on carbon film electrodes (CFEs) modified with carbon nanotubes (CNT) by electropolymerisation using potential cycling. Voltammetric and electrochemical impedance characterisation were performed. Glucose oxidase and uricase, as model enzymes, were immobilised on top of PBG/CNT/CFE and PTH/CNT/CFE for glucose and uric acid (UA) biosensing. Amperometric determination of glucose and UA was carried out in phosphate buffer pH 7.0 at −0.20 and +0.30 V vs. SCE, respectively, and the results were compared with other similarly modified electrodes existing in the literature. An interference study and recovery measurements in natural samples were successfully performed, indicating these architectures to be good and promising biosensor platforms.

1. Introduction

The selection and development of active sensing materials for electrodes is a big challenge for the construction of electrochemical biosensors. By using nanotechnology, a large number of new materials and devices of desirable properties can be designed and it is possible to control the fundamental properties of materials without changing the chemical composition. Complex nanobiosensor architectures can aid in performing continuous monitoring as implantable devices and in high throughput analysis such as lab-on-chip devices for rapid and low-cost screening of physiological metabolites [1].

Carbon nanotubes (CNT) have been extensively used in recent years due to their low cost, excellent chemical stability, good mechanical strength and electrical conductivity, good electron transfer kinetics and biocompatibility [2]. CNT can improve electrochemical properties, provide electrocatalytic activity and minimise electrode surface fouling, reasons that make them excellent materials for the development of electrochemical sensors and biosensors [3–5], generally leading to higher sensitivities and lower detection limits than traditional electrode materials.

Conducting polymers (CP) have also been extensively studied as electroactive materials during recent decades. Among them, redox dye polymers, especially phenazine derivatives, have had many applications in sensors and biosensors (e.g. [6–9]).

CP/CNT nanocomposite modified electrodes have received significant interest because the incorporation of conducting polymers into CNT can lead to new composite materials possessing the properties of each component, with a synergistic effect that would be useful in specific applications [10]. Carbon nanotubes can improve the conductivity of conducting polymer matrices and form a three-dimensional network which can facilitate access to the analyte and increase the rate of electron transfer [11].

The determination of both glucose and uric acid is of great clinical importance. Uric acid is related to gout, cardiovascular and renal diseases, leukaemia and pneumonia [12] and a high glucose level is associated with diabetes, which is related to complications to retina, the circulatory system and kidneys [1]. New strategies based on different nanomaterials, nanostructures or nanotechnologies for the development of biosensors have been explored for the determination of these compounds, electrochemical ones often being preferred [1,13–16].

In the present work, nanostructured composites have been prepared by electropolymerisation of brilliant green (BG) and thionine (TH) (see Scheme 1), onto CNT-modified carbon film electrodes (CFE). The modified electrodes PBG/CNT/CFE and PTH/CNT/CFE served as platforms for the immobilisation of glucose oxidase (GOx) and uricase (UOx) which were used for sensing glucose and uric acid. To our knowledge, thionine monomer and carbon nanotubes have been only used once to develop uric acid [17] and glucose [18] biosensors; however, in both studies thionine

* Corresponding author. Tel.: +351 239854470; fax: +351 239827703.
E-mail address: cbrett@ci.uc.pt (C.M.A. Brett).

http://dx.doi.org/10.1016/j.talanta.2014.06.068
0039-9140/

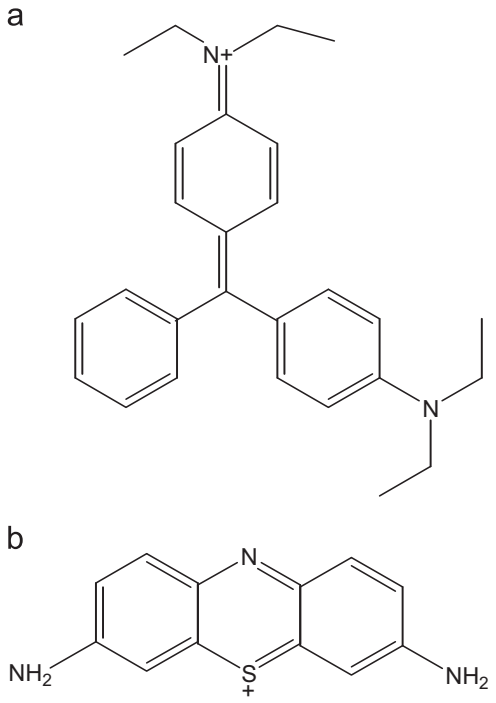

Scheme 1. Chemical structure of monomers (a) brilliant green and (b) thionine.

was not polymerised and, in the case of glucose, the biosensor also contained platinum nanoparticles. Regarding carbon nanotubes and poly(brilliant green), there is no report up until now either for glucose, or for uric acid determination. A comparison between the performances of the developed biosensors under the same conditions was performed, the results are discussed with respect to other sensors in the literature and natural samples are analysed.

2. Experimental

2.1. Reagents and solutions

All reagents were of analytical grade and were used without further purification. Glucose oxidase (GOx, E.C. 1.1.3.4, from *Aspergillus niger*, 24 U/mg), uricase (UOx, E.C. 1.7.3.3, from *Bacillus fastidiosus*, 16.2 U/mg), phenol and brilliant green (BG) were acquired from Fluka. α-D(+)-glucose, uric acid (UA), L-ascorbic acid (AA), glutaraldehyde (GA) (25% v/v in water), bovine serum albumin (BSA) and urea were purchased from Sigma. Citric acid, creatinine and ammonia were from Merck. Multi-walled carbon nanotubes (MWCNT) were from NanoLab, U.S.A., with ~95% purity, 30 ± 10 nm diameter and 1–5 μm length. Chitosan (Chit) of low molecular weight with a degree of deacetylation of 80% and thionine (TH, dye content 90%) were obtained from Aldrich.

All solutions were prepared using Millipore Milli-Q nanopure water (resistivity > 18 MΩ cm). The supporting electrolyte for biosensors evaluation was sodium phosphate buffer saline, NaPBS (0.1 M NaH_2PO_4/Na_2HPO_4 + 0.05 M NaCl), pH 7.0. For BG electropolymerisation, universal buffer McIlvaine (0.1 M citric acid + 0.2 M Na_2HPO_4) pH 4.0 was used and for TH polymerisation the buffer was sodium tetraborate (0.025 M $Na_2B_4O_7$) + 0.10 M KNO_3, pH 9.0.

2.2. Methods and instruments

All measurements were performed in a 15 mL, one-compartment, cell containing a carbon film electrode (CFE) as working electrode, a platinum wire auxiliary electrode and a saturated calomel electrode (SCE) as reference.

Voltammetric and amperometric experiments were carried out using a CV-50 W Voltammetric Analyser from Bioanalytical Systems, controlled by BAS CV-2.1 software.

The pH measurements were performed with a CRISON 2001 micro-pH-meter. All experiments were performed at room temperature, 25 ± 1 °C.

2.3. Carbon film electrode preparation and pre-treatment

The working electrodes were made from carbon film resistors (2 Ω nominal resistance, 15 μm film thickness) of length 6 mm and 1.5 mm in diameter; the detailed preparation is described elsewhere [19]. The cylindrical resistor, a carbon film pyrolitically deposited on a ceramic substrate, has two tight-fitting metal caps, one at each end, linked to an external contact wire. In order to make the electrode one of them was removed and the other shielded in plastic and protected by normal epoxy resin. The exposed geometric area of the electrodes is 0.20 cm^2.

Since carbon film electrode surfaces cannot be renewed by polishing or other mechanical methods, electrochemical pretreatment was always performed before use in order to achieve a reproducible electrode response. This consisted in potential cycling between −1.0 and +1.0 V vs. SCE, at 100 mV s^{-1}, until a stable voltammogram was obtained.

2.4. Carbon nanotube functionalisation and deposition

Multi-walled carbon nanotubes (MWCNT) were purified and functionalised as previously described [20]. A mass of 120 mg of MWCNT was stirred in 10 mL of a 5 M nitric acid solution for 24 h, in order to cause partial destruction of the CNTs and introduce –COOH groups at the ends and sidewall defects of the CNT [21]. The solid product was collected on a filter paper and washed several times with nanopure water until the filtrate solution became neutral (pH ≅ 5). The functionalised MWCNT were then dried in an oven at 80 °C for 24 h.

In order to prepare a 1.0% w/v chitosan solution, 100 mg of Chit powder was dissolved in 10 mL of 1.0% v/v acetic acid solution and stirred for 3 h at room temperature to ensure complete dissolution. The chitosan solution was stored at 4 °C.

A 1.0% w/v MWCNT solution was prepared by dispersing 3 mg of functionalised MWCNT in 300 μL of 1.0% w/v Chit in 1.0% v/v acetic acid solution and sonicating for 3 h. For CNT deposition a 10 μL drop of the 1% w/v MWCNT solution was placed on the surface of the CFE, left to dry in air at room temperature and this step was then repeated.

2.5. Brilliant green and thionine polymerisation

Poly(brilliant green) (PBG) and poly(thionine) (PTH) films were formed by electropolymerisation using potential cycling.

Prior to polymerisation of BG, the electrode was activated, as described in [22] for malachite green, by cycling in 0.1 M sulphuric acid between −1.0 and +2.0 V vs. SCE at 100 mV s^{-1} until a stable voltammogram was obtained. Polymerisation of BG was carried out in an aqueous solution containing 1 mM brilliant green in McIlvaine buffer, pH 4.0, sweeping the potential between −1.0 and +1.2 V at a scan rate of 100 mV s^{-1} during 5 cycles [23] at CFE and 20 cycles at CNT/CFE.

For TH polymerisation, a solution of 0.025 M $Na_2B_4O_7$ + 0.10 M KNO_3, pH 9.0 and 1 mM thionine was used. Polymerisation of thionine can occur from different media [24,25]; these studies point to a higher pH value for better film growth, as occurs with other phenothiazines [26]. Potential cycling polymerisation was

done between −1.0 and +1.0 V vs. SCE at a scan rate of 50 mV s^{-1} during 30 cycles at CFE and 40 cycles at CNT/CFE.

2.6. Enzyme immobilisation

A glucose oxidase solution was prepared by dissolving 10 mg GOx and 40 mg BSA in 1 mL of 0.1 M NaPBS (pH 7.0). Each 10 μL of the previous solution was mixed with 5 μL of GA (2.5% v/v in water) and from this mixture a volume of 10 μL was placed onto the previously modified electrodes PBG/CNT/CFE or PTH/CNT/CFE. The uricase solution was prepared by dissolving 5 mg of UOx in 1 mL of 0.1 M NaPBS (pH 7.0) and then placing 10 μL of this solution onto the carbon nanotube/polymer modified electrodes. When not in use, enzyme electrodes were kept in phosphate buffer electrolyte, pH 7.0 at 4 °C.

3. Results and discussion

3.1. Carbon nanotube/polymer deposition and characterisation

Among the preparation methods of polymer/nanotube composites, a simple one and maybe the most used is polymerisation of the corresponding monomer after modification by carbon nanotubes [27–29].

Poly(brilliant green) and poly(thionine) were deposited by potential cycling onto carbon film electrodes or on CFE modified with carbon nanotubes; cyclic voltammograms obtained during polymerisation are shown in Fig. 1. For brilliant green at CFE, Fig. 1a inset, three oxidation and four reduction peaks were observed. At high positive potentials, ~1.0 V vs. SCE, irreversible monomer oxidation occurs, BG_1. At 0.8 V appears a redox couple BG_{2a}/BG_{2c}. Since BG_1 decreases in height with each cycle and BG_{2a} increases, while BG_{2c} decreases, this couple can be associated with an intermediary form of partially oxidised monomer [23] which is probably not very stable at this pH. The monomer reduction peak, BG_{3c} at CNT/CFE, appears as a double peak at CFE, probably due to the same intermediate forms mentioned. With more cycles, these two peaks decrease in height and overlap, finally transforming to one peak, similarly to CNT/CFE. The redox couple, PBG_{1a}/PBG_{1c} with formal potential 0.37 V is due to polymer oxidation/reduction and its height increases with each cycle, showing poly(brilliant green) growth.

Thionine polymerisation (Fig. 1b), exhibited similar cyclic voltammograms at bare and carbon nanotube modified carbon film electrodes. Monomer cation radical formation occurs close to +1.0 V. Two redox couple are visible, the more negative one, midpoint potential −0.237 V at CFE and −0.320 V at CNT/CFE is ascribed to monomer oxidation/reduction, TH_{1a}/TH_{1c}, and the other, ~0.05 V at CFE and 0.115 V at CNT/CFE is due to oxidation and reduction of the polymer, PTH_{1a}/PTH_{1c}. The monomer couple peaks decrease with each cycle, while those of the polymer increase, indicative of poly(thionine) growth.

The PBG film is deposited faster at CNT/CFE than PTH: peak currents increased up to 20 cycles for PBG, whereas for PTH, the film stopped growing only after 40 cycles. This can be attributed to continued brilliant green monomer diffusion to all nucleation sites within the CNT network on the surface (see Fig. 2) as well as the increased surface area. At bare electrodes (see inset of Fig. 1) the polymerisation of brilliant green stops very quickly, after 5 scans, whereas thionine continues to be polymerised up to 30 cycles.

The mechanism of polymerisation of brilliant green has been previously discussed [23] and details concerning thionine polymerisation can also be encountered [30]. During polymerisation, as observed in the cyclic voltammograms, as well as visually after polymerisation, a better polymer film is formed by PTH on bare

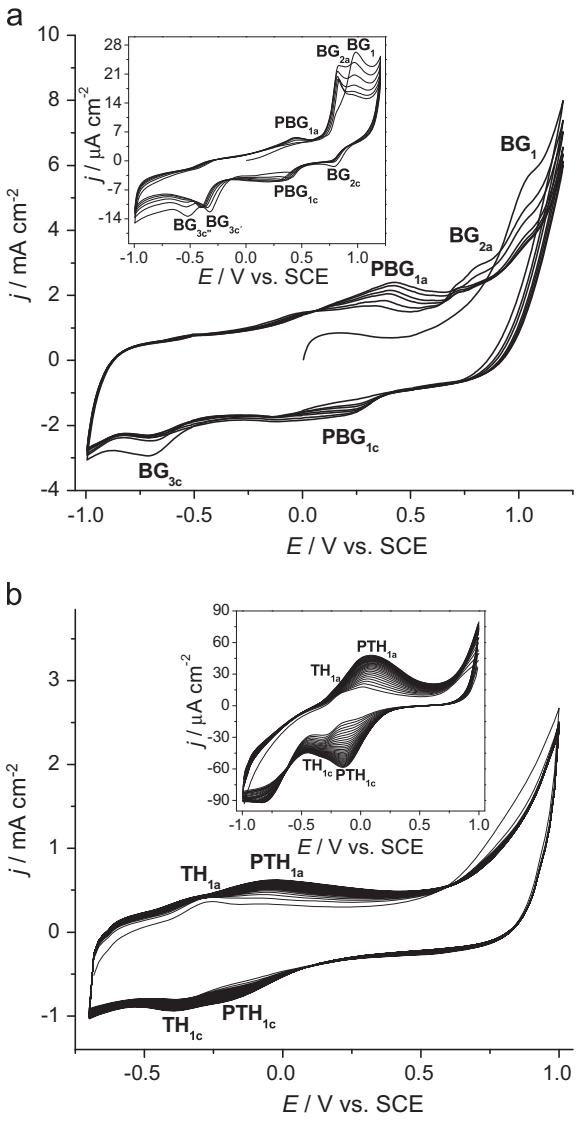

Fig. 1. Cyclic voltammetry for polymerisation at CNT/CFE of (a) 1.0 mM BG at 100 mV s^{-1} in McIlvaine buffer pH 4.0 and (b) 1.0 mM TH at 50 mV s^{-1} in 0.025 M $Na_2B_4O_7$ + 0.10 M KNO_3, pH 9.0. Insets show polymerisation under the same conditions at CFE.

carbon film electrodes, whereas at carbon nanotube modified carbon film electrode, PBG is better. This is probably due to the more flexible chemical structure of the brilliant green monomer, as can be verified in Scheme 1, compared with that of thionine, which makes entry of BG into the carbon nanotube structure easier. In both cases the polymer redox couple current peaks increased greatly in the presence of nanotubes. This effect can be attributed to the large number of defects and spatial nanostructure of nanotubes that can act as a molecular wire and enhance electron transfer [30].

The modified electrodes PBG/CFE, PTH/CFE, PBG/CNT/CFE and PTH/CNT/CFE were characterised by cyclic voltammetry (CV), electrochemical impedance spectroscopy (EIS) and scanning electron microscopy (SEM). The scanning electron micrographs showed similar morphologies for the polymer modified electrodes (Fig. 2b1 and c1) and the unmodified electrode (Fig. 2a1), meaning that the covering layer is very thin. The presence of peaks in cyclic voltammetry (Fig. 2b2 and c2) indicates the presence of some polymer on the bare carbon film electrode. Regarding the CNT-modified electrodes, the electrode surface is uniformly covered by the nanotubes and the two polymers grow in different ways on

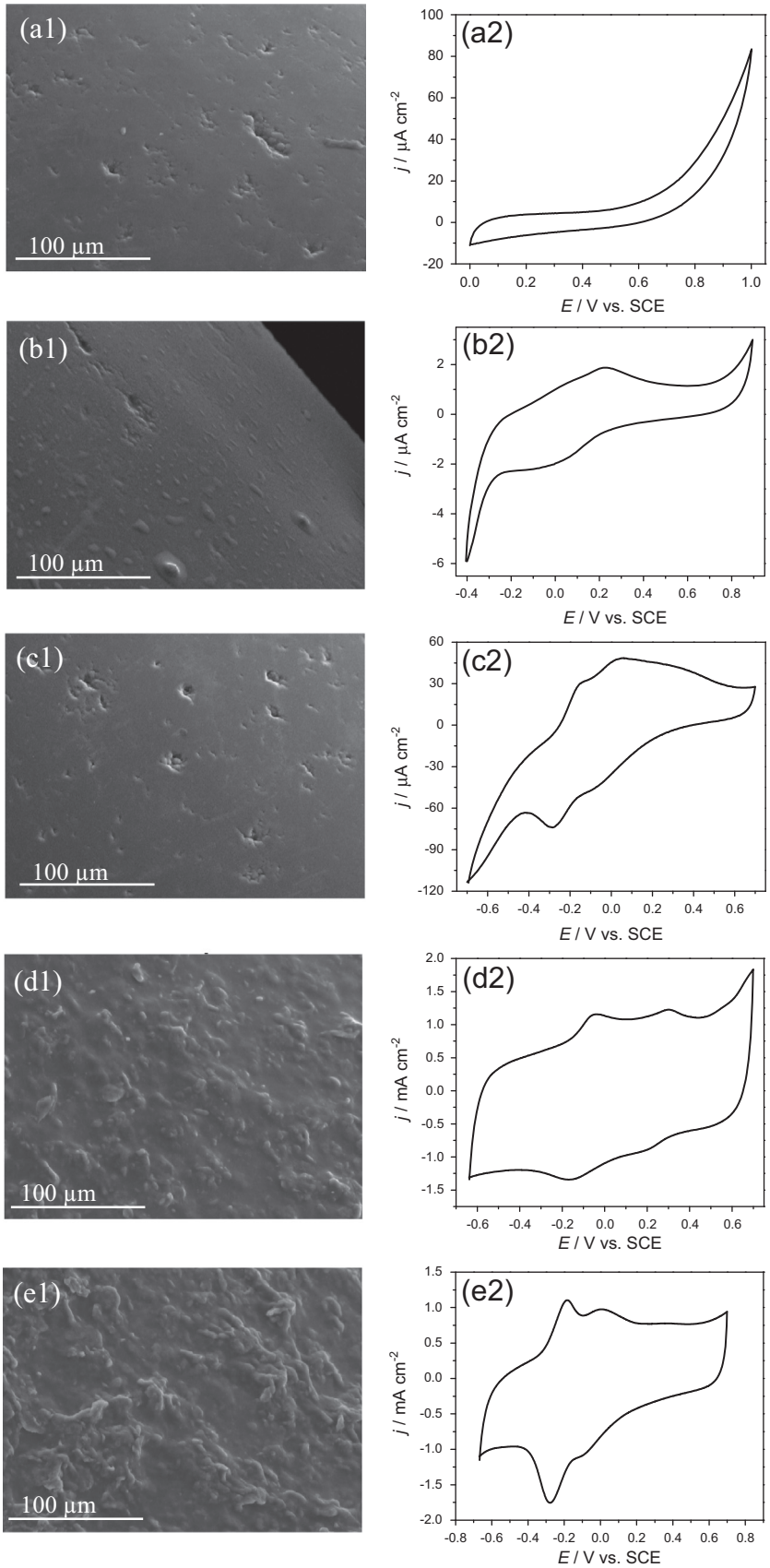

Fig. 2. Scanning electron micrographs of (a1) CFE, (b1) PBG/CFE, (c1) PTH/CFE, (d1) PBG/CNT/CFE and (e1) PTH/CNT/CFE and (a2)–(e2) their respective cyclic voltammograms in 0.1 M NaPBS pH 7.0.

them. In the case of thionine, which has a more planar structure, the polymer covers the CNT surface, PTH growing over the nanotubes, forming a distinct and rough layer, as can be observed from the thick structures formed on top of CNT in Fig. 2e1. On the other hand, brilliant green, a more flexible molecule, can enter inside the nanotubes and form a nanostructured composite, as discussed above for the electropolymerisation CVs: more homogeneous and thinner structures above are observed in Fig. 2d1.

Impedance spectra recorded at 0.0 V vs. SCE for bare carbon film electrodes, carbon nanotube, polymer and carbon nanotube/polymer modified electrodes are shown in Fig. 3. All spectra, except at the bare electrode, present a semicircle in the high frequency region, corresponding to the electron transfer process, and a linear low frequency region, due to diffusion. The bare electrode spectrum shows only the linear part, consistent with no electron transfer occurring at this potential. The generic electrical circuit used to model the spectra consists of a cell resistance, R_Ω, in series with a parallel combination of a charge transfer resistance, R_{ct}, and a constant phase element, CPE_{dl}, representing the electrode/solution interface, this in series with a parallel combination of a resistance, R_f, and a second constant phase element, CPE_f, representing the film. Only polymer modified electrodes required inclusion of R_f (Fig. 4b) in the equivalent circuit and for bare electrodes the circuit consisted only of R_Ω and CPE_{dl} (Fig.4a). The constant phase elements are modelled as non-ideal capacitors and are described by $CPE = -(i\omega C)^{-\alpha}$, where ω is the angular frequency and α the CPE exponent, reflecting a non-uniform surface.

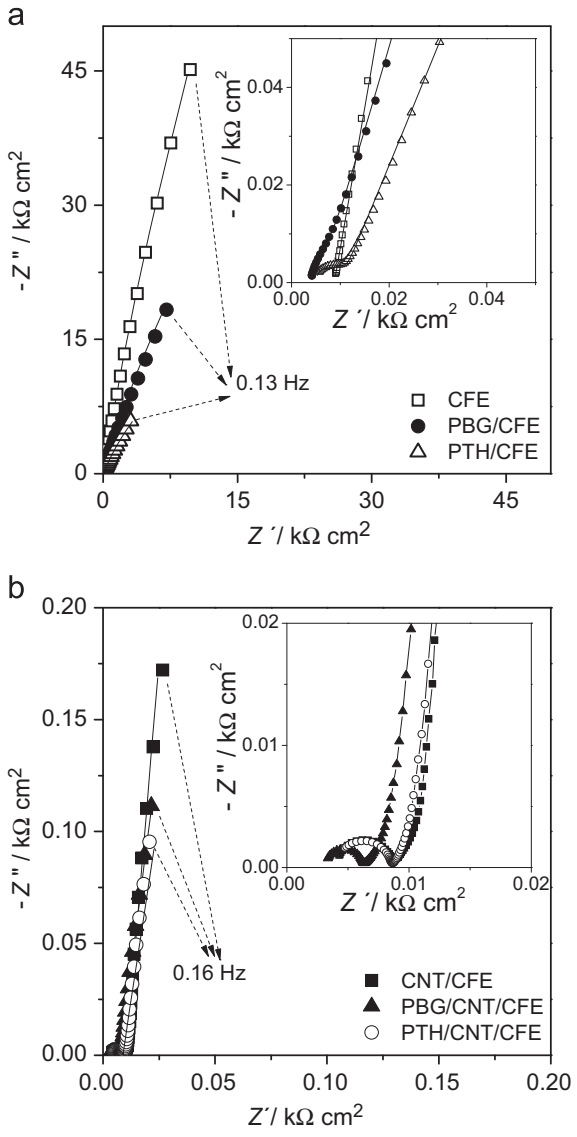

Fig. 3. Complex plane impedance spectra for different electrodes (a) CFE (□), PBG/CFE (•), PTH/CFE (Δ) and (b) CNT/CFE (■), PBG/CNT/CFE (▲), PTH/CNT/CFE (○) at 0.0 V vs. SCE in 0.1 M NaPBS, pH 7.0. Insets are the magnifications of the high frequency portion. Lines show equivalent circuit fitting (see Fig.4 for electrical circuits).

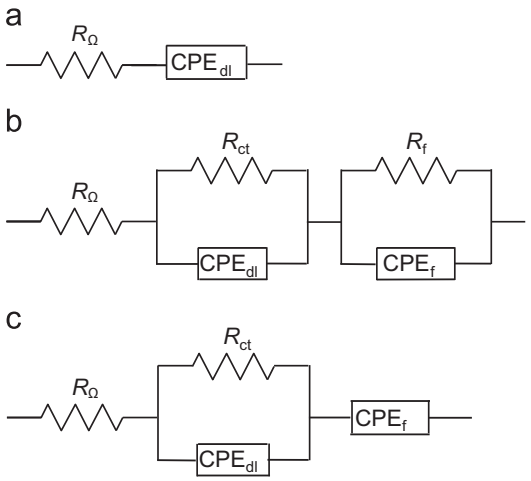

Fig. 4. Equivalent circuits used for fitting the spectra of (a) CFE, (b) PBG/CFE and PTH/CFE and (c) CNT/CFE, PBG/CNT/CFE and PTH/CNT/CFE.

Table 1
Data obtained from equivalent circuit fitting of the impedance spectra for the bare and modified electrodes in 0.1 M NaPBS at pH 7.0.

Electrode	R_{ct} (Ω cm^2)	CPE_{dl} (μF cm^{-2} s$^{\alpha-1}$)	α_1	R_f (kΩ cm^2)	CPE_f (mF cm^{-2} s$^{\alpha-1}$)	α_2
CFE	–	17.0	0.90	–	–	–
PBG/CFE	220	32.8	0.82	2.7	0.03	0.92
PTH/CFE	7.4	28.3	0.73	47	0.19	0.76
CNT/CFE	6.2	99.6	0.71	–	7.3	0.92
PBG/CNT/CFE	4.4	97.0	0.69	–	14.0	0.88
PTH/CNT/CFE	5.9	30.6	0.73	–	10.5	0.91

Calculated values of the circuit parameters are shown in Table 1. The values of R_Ω were between 4 and −8 Ω cm^2, the R_{ct} value is much higher for PBG/CFE compared with that for PTH/CFE, which is in agreement with lower currents in cyclic voltammetry, since less polymer was deposited. Moreover, at the potential studied, 0.0 V, only a small redox activity of PBG is observed. On the other hand, the film resistance R_f, is smaller for PBG, and this might be related to faster diffusion of counterions through this film.

The value of the charge transfer resistance decreased when the electrodes were modified by nanotubes, corresponding to easier electron transfer. A further small decrease was observed with addition of polymers, meaning that the rate of electron transfer is mainly dictated by the nanotubes. In the presence of CNT, the value of R_{ct} is smaller for the PBG/CNT modified electrode, meaning that electron transfer is easier and suggests that PBG is more easily deposited on the CNT than is PTH; as found below in the application as biosensor, this modified electrode shows a better performance. The double layer capacitance, expressed as CPE_{dl}, is higher for modified electrodes than bare, while α_1 decreases, due to the less uniform surface. With CNT and polymer/CNT, the values are much higher and with similar values of α_1. The CPE_{dl} value for PBG/CNT/CFE is similar to that of CNT/CFE, which corroborates

what was stated above, that PBG is deposited within the CNT structure; hence, the interface is more similar to CNT only. On the other hand the PTH/CNT/CFE and PTH/CFE interfaces are alike, as reflected by the similar CPE_{dl} values.

In the presence of CNT, the modifier layer offers no resistance, only charge separation, CPE_f, the value of which increases with each layer of modifier, being highest for PBG/CNT/CFE. This confirms the results obtained by cyclic voltammetry where the highest capacitive currents were observed for PBG/CNT/CFE (see Fig. 2d2 and e2).

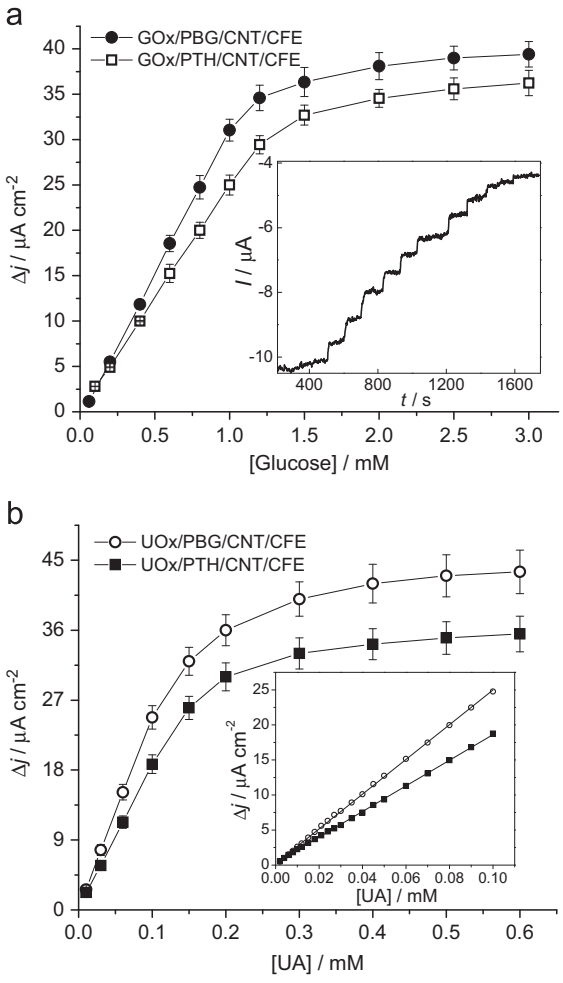

Fig. 5. Calibration curves for (a) glucose at (•) GOx/PBG/CNT/CFE and (□) GOx/PTH/CNT/CFE biosensors at −0.20 V and (b) for UA at (○) UOx/PBG/CNT/CFE and (■) UOx/PTH/CNT/CFE biosensors at +0.30 V vs. SCE in 0.1 M NaPBS, pH 7.0. Inset shows (a) typical response at glucose biosensor and (b) linear range for uric acid.

3.2. Glucose biosensor

The modified electrodes GOx/PBG/CNT/CFE and GOx/PTH/CNT/CFE were employed for the determination of glucose by fixed potential amperometry. The effect of applied potential on the current response as a function of glucose concentration was studied. Amperometric measurements were performed at potentials ranging from −0.20 to +0.10 V under continuous stirring, glucose being injected after baseline stabilisation. The results obtained are shown in Fig. 5a as calibration curves, Δj corresponding to the change in current density. In the range of applied potentials studied, anodic currents were observed at all potentials at both GOx/PBG/CNT/CFE and GOx/PTH/CNT/CFE. It has been previously shown that binding of glucose oxidase to high molecular redox polymer results in the establishment of direct electrical communication between the redox centre of the enzyme and the electrode, different polyphenazines exhibiting this behaviour [31,32]. The mechanism proposed is similar to that in [13,28,31], attributed to competition between FAD regeneration and hydrogen peroxide reduction. For both electrodes the response decreases when moving to more positive potentials; hence, the best choice was to determine glucose at −0.20 V vs. SCE. The analytical parameters obtained are shown in Table 2 together with those of some recent, similar biosensors in the literature.

Examination of Table 2 shows that the applied potential of the new biosensor is less negative than many others previously reported [28,33–35]. Although one biosensor has a much higher sensitivity than that obtained here [18], based on thionine adsorbed on MWCNT, together with platinum nanoparticles, that greatly enhance the response, it operates at a much higher potential of +0.50 V vs. SCE. Biosensors based on a carbon film electrode modified with poly(neutral red)/CNT [28] and on a poly (3,4-ethylenedioxythiophene)/CNT modified carbon cloth electrode [33] showed similar sensitivities at −0.30 V vs. SCE; however, all the others [28,34–37] exhibited lower responses than the biosensor proposed here.

The storage stability of the biosensors was checked every 3 days over a period of one month by performing a calibration curve consisting of 10 injections each time. When not in use, the electrodes were kept in phosphate buffer at 4 °C. In the case of the GOx/PBG/CNT/CFE biosensor, a decrease of 18% from the initial response was observed, whilst for GOx/PTH/CNT/CFE the response dropped by 30%. The reproducibility of the biosensors was assessed by comparing the sensitivity for 4 different electrodes prepared in the same way. The relative standard deviation of the

Table 2
Comparison of analytical parameters for glucose biosensors at different modified electrodes.

Electrode	Potential (V) vs. reference	Linear range (mM)	Sensitivity (μA mM^{-1} cm^{-2})	LOD (μM)	Reference
GOx/PtNPs-TH-MWCNT/Au	+0.50 (SCE)	0.001–11.1	140	0.05	[18]
GOx/PNR/CNT/GCE	−0.30 (SCE)	0.2–1.6	30.4	17	[28]
GOx/PBCB/CNT/GCE	−0.30 (SCE)	0.2–1.6	10.1	14	[28]
GOx/PEDOT/CNT-CCl	−0.30 (SCE)	0.2–1.2	33.4	0.065	[33]
GOx/RGO/GCE	−0.447 (Ag/AgCl)	0.1–27	1.85	[a]	[34]
GOx/ZnO/GOx/MWCNT/GCE	−0.30 (SCE)	0.0067–1.29	10.0	2.22	[35]
GOx-PTBO/CNT/GCE	−0.10 (Ag/AgCl)	1.0–7.0	14.5	[a]	[36]
GOx/CS-PPy/GCE	+0.132 (SCE)	0.5–147	3.34	15.5	[37]
GOx/PBG/CNT/CFE	−0.20 (SCE)	0.2–1.2	32.4	12	This work
GOx/PTH/CNT/CFE	−0.20 (SCE)	0.2–1.2	24.6	30	This work

Abbreviations: PtNPs, Pt nanoparticles; PNR, poly(neutral red); PBCB, poly(brilliant cresyl blue); PEDOT, poly(3,4-ethylenedioxythiophene); CCl, carbon cloth; RGO, reduced graphene oxide; PTBO, poly(toluidine blue O); CS-PPy, chitosan-polypyrrole.

[a] Not specified.

response (RSD) was 2.4% for GOx/PBG/CNT/CFE and 4% for GOx/PTH/CNT/CFE indicating a reproducible fabrication method. Similarly, to evaluate the repeatability of the biosensors, the RSD was calculated for 6 successive measurements of glucose. In this process, the electrode was regenerated by immersing in phosphate buffer, pH 7.0, after each measurement. The values of RSD were 3.5% and 3.3% for GOx/PBG/CNT/CFE and GOx/PTH/CNT/CFE biosensors.

3.3. Uric acid biosensor

Cyclic voltammetry at a bare carbon film electrode showed that oxidation of uric acid occurs at +0.58 V vs. SCE (Fig. 6 inset). When electrodes were modified with PBG/CNT and PTH/CNT, the value of the oxidation peak potential was shifted negatively by more than 200 mV in each case, to +0.34 and +0.32 V, respectively, a good indication that the mediators used are good electrocatalysts for uric acid oxidation.

The influence of the applied potential on the response of the UOx/PBG/CNT/CFE and UOx/PTH/CNT/CFE biosensors was examined in the range −0.20 V to +0.40 V vs. SCE. In all cases oxidation currents were observed, most probably due to mediator re-oxidation at the electrode surface. The maximum current value obtained was at +0.20 V for UOx/PTH/CNT/CFE and at +0.35 V for UOx/PBG/CNT/CFE. The difference is probably due to the fact that the mediators used have slightly different redox couple potentials as seen in Fig. 2d2 and e2. In order to enable a comparison under the same conditions, a compromise value of +0.30 V was chosen as the potential to apply in fixed potential amperometry.

A comparison between the response to uric acid at CFE, PBG/CNT/CFE, PTH/CNT/CFE, UOx/PBG/CNT/CFE and UOx/PTH/CNT/CFE

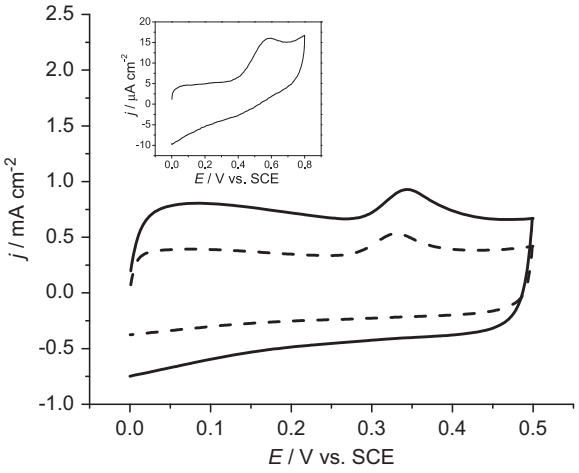

Fig. 6. Cyclic voltammetry for 0.60 mM UA in 0.1 M NaPBS pH 7.0 at PBG/CNT/CFE (solid line) and PTH/CNT/CFE (dash); scan rate 50 mV s^{-1}. Inset shows the response at bare CFE.

was made under the same experimental conditions. The response at the bare electrode was around 130 and 170 times lower than UOx/PTH/CNT/CFE and UOx/PBG/CNT/CFE, respectively, and the electrodes modified with PTH/CNT/CFE and PBG/CNT/CFE exhibited 4 and 5 times lower sensitivity. Although at the applied potential used, some direct oxidation of uric acid at bare electrode occurs, the results clearly showed that the presence of enzyme greatly increases the response.

Calibration curves for the response to uric acid at UOx/PTH/CNT/CFE and UOx/PBG/CNT/CFE are shown in Fig. 5b and it is seen that the behaviour is similar, with a linear range up to 100 μM and submicromolar detection limits. However, the electrode with PBG exhibited a higher response. A comparison with other uricase based biosensors in similar configurations as those here, the modifier layer containing CNT and polymers, was made (see Table 3). The sensitivity obtained with the proposed biosensors is not as high as that reported at gold electrodes modified with MWCNT operating at a higher potential of +0.4 V with either Prussian blue, or gold nanoparticles [14,15]; however, the detection limits of 5 μM [14] and 10 μM [15] were much higher than here. A similar detection limit, 0.5 μM, was achieved at GCE modified with thionine adsorbed on single wall CNT, UOx-Th-SWCNT/GCE [17], but the sensitivity was much lower than that obtained with either of the biosensors proposed here. Another uricase biosensor, containing thionine and graphene oxide at glassy carbon electrode UOx/T-GOs/GCE [38] did not exhibit a higher response than here (5.3 nA cm^{-2} μM^{-1}) and the detection limit, 7 μM, was much higher.

Long term biosensor stability was assessed by constructing a calibration curve from 10 injections every 3 days, storing in phosphate buffer at 4 °C when not in use. After 6 weeks, 70% of the initial response was found with UOx/PBG/CNT/CFE and 60% with the UOx/PTH/CNT/CFE biosensor. The stability is better than that reported in [39], where the response dropped to 79.5% after 20 days of intermittent use, storing at 4 °C, or in [15] where the electrode showed 75% response after 45 days when used every 5 days, but less good than at UOx/PBNPs/MWCNT/PANI/Au [14], which maintained 60% of the initial activity after 7 months of weekly usage. However, and very interestingly, after 7 months storage in buffer at 4 °C the response of both uricase biosensors developed here remained the same as after 6 weeks.

Biosensor repeatability was tested by constructing three successive calibration curves and the relative standard deviation was 2.7% for UOx/PBG/CNT/CFE and 3.3% for UOx/PTH/CNT/CFE. The reproducibility between three different electrodes was assessed by comparing the sensitivity under the same conditions and the RSD was 3.0% and 3.8%, respectively, for the two biosensors.

3.4. Interferences and determination in natural samples

Interference studies were conducted by placing the modified electrodes in buffer solution, under continuous stirring. After

Table 3
Comparison of analytical parameters for uric acid biosensors at different modified electrodes.

Electrode	Potential (V) vs. reference	Linear range (μM)	Sensitivity (nA cm^{-2} μM^{-1})	LOD (μM)	Reference
UOx/PBNPs/MWCNT/PANI/Au	+0.40 (Ag/AgCl)	5.0–80	1274	5.0	[14]
UOx/AuNP/MWCNT/Au	+0.40 (Ag/AgCl)	10–800	5866	10	[15]
UOx/ZnO/MWCNT/PG	+0.32 (SCE)	5.0–1000	393	2.0	[16]
UOx-Th-SWCNT/GCE	−0.40 (SCE)	2.0–2000	90	0.5	[17]
UOx/T-GOs/GCE	−0.25 (SCE)	20 to −4500	5.0	7.0	[38]
UOx/MWCNT/SnO_2/GCE	+0.25 (SCE)	0.1–500	345	0.05	[39]
UOx/PBG/CNT/CFE	+0.30 (SCE)	2.0–100	248	0.6	This work
UOx/PTH/CNT/CFE	+0.30 (SCE)	2.0–100	182	0.8	This work

Abbreviations: PBNP, Prussian Blue nanoparticles; PANI, polyaniline; AuNP, Au nanoparticles; PG, pyrolytic graphite; T-GOs, thionine-graphene oxide.

waiting for the baseline current to stabilise, the analyte was injected, followed by the interferents and, finally, the same amount of analyte was injected again.

Measurements in samples were performed by standard addition, first adding the sample, followed by 4 additions of analyte standard and determining the concentration of sample from the linear regression parameters.

3.4.1. Glucose

Compounds usually present in matrices where glucose is determined such as ascorbic acid, uric acid, dopamine and fructose were tested as potential interferents, using the same concentration of glucose and interferents, 0.20 mM. No change in response was observed from the tested compounds at either GOx/PBG/CNT/CFE or GOx/PTH/CNT/CFE biosensors, thus showing a very high selectivity towards glucose.

In order to check the precision and accuracy of the glucose biosensor, GOx/PBG/CNT/CFE and GOx/PTH/CNT/CFE were applied to glucose determination in serum containing glucose (labelled with 5.5 mg glucose per 100 mL). The sample acquired from the local pharmacy was used as received and the determination of glucose was carried out by the standard addition method: first, injection of the serum, followed by 4 additions of standard glucose of 0.1 or 0.2 mM. Three different concentrations were analysed in triplicate and the values are shown in Table 4. Good recoveries ranging from 94% to 97% were obtained, which is encouraging for application to natural samples.

3.4.2. Uric acid

For the interference study, different compounds usually found in human urine [40] were tested, i.e. ammonia, ascorbic acid, creatinine, citric acid, glucose, phenol and urea. The concentration of the interferents was 10 times higher than that of uric acid. Only ascorbic acid responded, its presence inducing a 20% and 25% increase in UOx/PBG/CNT/CFE and UOx/PTH/CNT/CFE biosensor current response. However, in human urine the ascorbic acid level is about 13 times lower than that of uric acid; hence, it should not be a problem for determination by the standard addition method.

Urine samples from two healthy volunteers were analysed for uric acid and the values found were 3.66 ± 0.040 and 4.17 ± 0.035 mM with UOx/PBG/CNT/CFE and 3.45 ± 0.035 and 4.05 ± 0.030 mM with the UOx/PTH/CNT/CFE biosensor, showing good agreement between the two biosensors, the values being in the normal range [41]. Recovery measurements were also performed by adding two different known concentrations to the urine samples and determination in triplicate was performed with good precision; the values obtained did not vary by more than 5% from those expected (Table 4).

Table 4
Recovery of glucose in pharmaceutical serum containing glucose and of uric acid in human urine samples.

Analyte	Biosensor	Added (mg)	Found (mg)	Recovery (%)
Glucose	GOx/PBG/CNT/CFE	27.5	26.1 ± 0.09	95
		55.0	52.4 ± 0.4	95
		110	103.6 ± 0.8	94
	GOx/PTH/CNT/CFE	27.5	26.7 ± 0.1	97
		55.0	52.9 ± 0.6	96
		110	105.0 ± 0.9	95
Uric acid	UOx/PBG/CNT/CFE	5.0	5.2 ± 0.03	104
		15	14.4 ± 0.09	96
	UOx/PTH/CNT/CFE	5.0	4.75 ± 0.04	95
		15	15.8 ± 0.1	105

4. Conclusions

Poly(thionine) and novel poly(brilliant green) have been formed onto multiwalled carbon nanotube modified carbon film electrodes. The nanostructures were evaluated as platforms for enzyme immobilisation with the aim of developing new biosensors. For glucose and uric acid measurement, PBG-based enzyme biosensors exhibited a better response than PTH-based enzyme biosensors, with a higher sensitivity and lower detection limit. The biosensors developed here operated at less negative potentials for glucose and less positive for uric acid determination than previously reported in the literature, and the analytical parameters obtained with enzyme/PBG/CNT modified electrodes were better than others achieved by other polymer/CNT based glucose and uric acid biosensors. Recovery measurements in pharmaceutical and natural samples showed promising results, leading to the conclusion that they can be successfully employed as electrochemical biosensors. Thus, these configurations can be profitably used for developing other enzyme based biosensors and exploring miniaturisation strategies.

Acknowledgements

Financial support from Fundação para a Ciência e a Tecnologia (FCT), Portugal, PTDC/QUI-QUI/116091/2009, POCH, POFC-QREN (co-financed by FSE and European Community FEDER funds through the programme COMPETE – Programa Operacional Factores de Competitividade under the projects PEst-C/EME/UI0285/2013 and CENTRO-07-0224-FEDER-002001 (MT4MOBI)) is gratefully acknowledged. M.E.G. thanks FCT for postdoctoral fellowship SFRH/BPD/36930/2007.

References

[1] V. Scognamiglio, Biosens. Bioelectron. 47 (2013) 12–25.
[2] X. Yang, B. Feng, X. He, F. Li, Y. Ding, J. Fei, Microchim. Acta 180 (2013) 935–956.
[3] C.B. Jacobs, M.J. Peairs, B.J. Venton, Anal. Chim. Acta 662 (2010) 105–127.
[4] S.K. Vashist, D. Zheng, K. Al-Rubeaan, J.H.T. Luong, F.S. Sheu, Biotechnol. Adv. 29 (2011) 169–188.
[5] C.Y. Li, E.T. Thostenson, T.W. Chou, Compos. Sci. Technol. 68 (2008) 1227–1249.
[6] R. Pauliukaite, M.E. Ghica, M.M. Barsan, C.M.A. Brett, Anal. Lett. 43 (2010) 1588–1608.
[7] A.C. Torres, M.E. Ghica, C.M.A. Brett, Electroanalysis 24 (2012) 1547–1553.
[8] S. Kakhky, M.M. Barsan, E. Shams, C.M.A. Brett, Electroanalysis 25 (2013) 77–84.
[9] H.Y. Huo, H.Q. Luo, N.B. Li, Microchim. Acta 167 (2009) 195–199.
[10] M. Mazloum-Ardakani, M.A. Sheikh-Mohseni, in: Mohammad Naraghi (Ed.), Carbon Nanotubes – Growth and Applications, InTech, 2011 (Chapter 15).
[11] Q. Gao, M. Sun, P. Peng, H. Qi, C. Zhang, Microchim. Acta 168 (2010) 299–307.
[12] D.I. Feig, D.-H. Fang, R.J. Johnson, New Engl. J. Med. 359 (2008) 1811–1821.
[13] M.E. Ghica, R. Pauliukaite, O. Fatibello-Filho, C.M.A. Brett, Sens. Actuator B—Chem. 142 (2009) 308–315.
[14] R. Rawal, S. Chawla, N. Chauhan, T. Dahyia, C.S. Pundir, Int. J. Biol. Macromol. 50 (2012) 112–118.
[15] C. Chauhan, C.S. Pundir, Anal. Biochem. 413 (2011) 97–103.
[16] Y. Wang, L. Yu, Z. Zhu, J. Zhang, J. Zhu, Anal. Lett. 42 (2009) 775–789.
[17] D. Chen, Q. Wang, J. Jin, P. Wu, H. Wang, S. Yu, H. Zhang, C. Cai, Anal. Chem. 82 (2010) 2448–2455.
[18] R. Yu, L. Wang, Q. Xie, S. Yao, Electroanalysis 22 (2010) 2856–2861.
[19] C.M.A. Brett, L. Angnes, H.-D. Liess, Electroanalysis 13 (2001) 765–769.
[20] C. Gouveia-Caridade, R. Pauliukaite, C.M.A. Brett, Electrochim. Acta 53 (2008) 6732–6739.
[21] M.N. Tchoul, W.T. Ford, G. Lolli, D.E. Resasco, S. Arepalli, Chem. Mater. 19 (2007) 5765–5772.
[22] X. Wang, N. Yang, Q. Wan, X. Wang, Sens. Actuator B—Chem. 128 (2007) 83–90.
[23] M.E. Ghica, Y. Wintersteller, C.M.A. Brett, J. Solid State Electrochem. 17 (2013) 1571–1580.
[24] E. Topçu, M. Alanyalıoglu, J. Appl. Polym. Sci. 131 (2014) 39686-1–39686-9.
[25] A.A. Karyakin, E.E. Karyakina, H.-L. Schmid, Electroanalysis 11 (1999) 149–155.
[26] M.M. Barsan, E.M. Pinto, C.M.A. Brett, Electrochim. Acta 53 (2008) 3973–3982.
[27] R. Carvalho, C. Gouveia Caridade, C.M.A. Brett, Anal. Bioanal. Chem. 398 (2010) 1675–1685.

[28] M.E. Ghica, C.M.A. Brett, Microchim. Acta 170 (2010) 257–265.
[29] J.A. Rather, S. Pilehvar, K.D.E. Wael, Analyst 138 (2013) 204–210.
[30] C. Deng, J. Chen, Z. Nie, M. Yang, S. Si, Thin Solid Films 520 (2012) 7026–7029.
[31] R. Pauliukaite, M.E. Ghica, M.M. Barsan, C.M.A. Brett, J. Solid State Electrochem. 11 (2007) 899–908.
[32] X. Xiao, B. Zhou, L. Zhu, L. Xu, L. Tan, H. Tang, Y. Zhang, Q. Xie, S. Yao, Sens. Actuat. B 165 (2012) 126–132.
[33] M.M. Barsan, R.C. Carvalho, Y. Zhong, X. Sun, C.M.A. Brett, Electrochim. Acta 85 (2012) 203–209.
[34] B. Unnikrishnan, S. Palanisamy, S.-M. Chen, Biosens. Bioelectron. 39 (2013) 70–75.
[35] F. Hu, S. Chen, C. Wang, R. Yuan, Y. Chai, Y. Xiang, C. Wang, J. Mol. Catal. B—Enzym. 72 (2011) 298–304.
[36] Y.-L. Yao, K.-K. Shiu, Electrochim. Acta 53 (2007) 278–284.
[37] Y. Fang, Y. Ni, G. Zhang, C. Mao, X. Huang, J. Shen, Bioelectrochemistry 88 (2012) 1–7.
[38] Z. Sun, H. Fu, L. Deng, J. Wang, Anal. Chim. Acta 761 (2013) 84–91.
[39] F.-F. Zhang, X.-L. Wang, C.-X. Li, X.-H. Li, Q. Wan, Y.Z. Xian, L.-T. Jin, K. Yamamoto, Anal. Bioanal. Chem. 382 (2005) 1368–1373.
[40] D.F. Putnam, Composition and Concentrative Properties of Human Urine, NASA Contractor Report, Washington, DC, July 1971.
[41] C. Zhao, L. Wan, Q. Wang, S. Liu, K. Jiao, Anal. Sci. 25 (2009) 1013–1017.